Proceedings of the 4th International Conference on Fluid Flow and Thermal Science (ICFFTS'23)
Lisbon, Portugal- December 07 - 09, 2023
Paper No.148
DOI: 10.11159/icffts23.148

Thermal and Hydraulic Performance of Finned Tube Heat Exchangers

Saksham Gupta[1], Dan Ewing[1], Chan Y. Ching[1]
[1]Department of Mechanical Engineering, McMaster University, Hamilton, Ontario CANADA L8S 4L7
guptas70@mcmaster.ca; dwewing@rogers.com; chingcy@mcmaster.ca

Abstract **-** This study numerically examines the heat transfer and pressure drop performance of finned tube heat exchangers with staggered and inline tube layouts for a range of tube pitch. The case where the heat exchanger is placed in a fully ducted airflow with no bypass is considered. Strong horseshoe vortices developed around the fin-tube junction in both cases, which was associated with high heat transfer. The simulations indicate that the performance reduces considerably for the staggered tube layout with an increase in the tube pitch, but a minimal difference for the inline tube arrangement. The effects of other geometrical parameters like fin pitch and the number of tube rows and the Reynolds number are determined. Correlations for the heat transfer and pressure drop for the fin and tube heat exchangers with an inline tube layout are developed based on 280 simulations for 70 different configurations. The proposed heat transfer correlation predicts the dataset to within ±8 percent and the friction factor correlation predicts the dataset to within ±10 percent. The mean deviations for the heat transfer and friction factor correlations are 4.3 percent and 5.4 percent.

Keywords**:** Plain fin and tube heat exchanger; heat transfer correlation; friction factor correlation

1. Introduction

Plain fin and tube heat exchangers are ubiquitous in many thermal engineering applications. These are relatively easy to fabricate and consists essentially of round tubes set in parallel flat plain fins. The tubes can be arranged inline or staggered, and several parameters, such as the tube and fin pitch and the number of tube rows can be changed to affect its performance. When the plate-fin and tube heat exchanger is cooled by air, it can be either through natural or forced convection. In the latter case, the heat exchanger can be in a fully ducted airflow or in a partially ducted system where there is a bypass flow around it. The airflow across the tubes and the fin-tube surface can be quite complex and will depend on the geometrical parameters and Reynolds number. In applications such as air conditioning and refrigeration systems, plate-fin and tube heat exchangers with smaller tube pitch (<2.5Do) are typically used. For power electronics cooling, however, flat plate finned tube heat exchangers with larger tube pitch (>2.5Do) are typically used. Most existing studies on the heat transfer and pressure drop, including development of correlations, have been for small tube-pitched heat exchangers. Thus, more comprehensive studies on heat exchangers with larger tube pitch are required for the design of heat exchangers typically used for power electronics cooling.

The flow within a fin and tube heat exchanger can be considered as a channel flow perturbed by the tubes. For the inline geometry, the flow between the plates is mainly affected by the first row of tubes and thereafter passes through the channel to the outlet making contact with only a small fraction of the remaining tubes. In the staggered tube arrangement, however, the flow circulates around each downstream tube. The heat transfer and friction factor for both the inline and staggered tube arrangements are affected by various geometrical parameters such as fin pitch, tube pitch, tube diameter and the number of tube rows [1-5]. The successive accelerating and decelerating regions along with the adverse pressure gradient can produce a three-dimensional vortical structure known as a horseshoe vortex system. Most of the heat transfer occurs upstream of the fin and tube junctions, and is strongly linked to these horseshoe vortices [6].

There have been extensive studies on the thermo-hydraulic characteristics of fully ducted fin and tube heat exchangers with a staggered tube configuration, but far less for the inline tube configuration. Most of the early work was experimental [1-9], but lately, there have been an increasing number of numerical studies [10-13]. McQuiston and Tree [7] was one of the first to experiment on two test samples with a fin pitch of 0.173 and 0.3 diameters with an outer tube diameter of 10.3 mm and an inlet velocity ranging from 0.5-5.9 m/s. Later, Rich [3,8] performed experiments on 14 samples and concluded that heat transfer was independent of the fin pitch and the pressure drop was independent of the number of tube rows. McQuiston

[9,10] established correlations for the heat transfer and pressure drop with a deviation of 10 percent and 35 percent, respectively, by combing the data of Rich [2, 3] with his data for a geometry with tube diameter of 9.96 mm and fin density from 4 to14. Gray and Webb [11] noted the poor accuracy of the correlation for the friction factor of McQuiston and proposed a correlation with an RMS difference for the heat transfer and pressure drop of 7.3 and 7.8 percent, respectively. The developed correlation, however, was valid only for larger diameter tubes with a large number of tube rows. Later, Wang et al. [5,12,13] summarized the various parametric effects on the heat exchanger performance and developed correlations for heat transfer and friction factor for a wider range of data with deviations of 7.5 and 8.3 percent, respectively. The correlation was valid for a staggered geometry with a tube diameter of 6.35 to 12.7mm, fin pitch of 1.19 to 8.7mm, transverse tube pitch of 17.7 to 31.55mm, longitudinal tube pitch of 12.4 to 27.5mm with the tube rows less than 6.

There has been a large number of numerical studies on plain finned tube heat exchangers over the last two decades. Bastani [14] carried out one of the first computational studies on a finned tube bank with an inline arrangement and showed details of the flow field. Yang et al. [15] conducted a numerical study on four-row finned tube banks with tube pitch less than 2.4 diameters and fin pitch less than 0.75 diameters and concluded that the heat transfer coefficient is independent of the number of tube rows if larger than four. They also found out that the heat transfer coefficient and the friction factor for staggered tube arrangement is 15-27 percent and 20-25 percent, respectively, higher than for the inline tube arrangement. Bhuiyan [1,2] conducted numerical studies of inline and staggered tube geometries with tube pitch less than 2.5 diameters and fin pitch less than 0.4 diameters. The results showed a 25-30 percent higher heat transfer coefficient for the staggered tube arrangement than the inline case but with more than a 40 percent higher friction factor.

The objective of this work is to numerically investigate the performance of staggered and inline tube geometries for tube pitch of 1.5 to 3.5 diameters for the fully ducted configuration. The effects of different geometrical parameters for the inline tube arrangement are determined and compared to the staggered arrangement. New correlations for the Colbourn j-factor and the friction factor for the inline tube arrangement with relatively high tube pitch are developed.

2. Problem description and numerical methods

Numerical simulations for the flow and heat transfer in plain fin and tube heat exchangers were performed for both the inline and staggered tube arrangements. Schematic views of the plate-fin and tube heat exchangers considered in this study are shown in Figure 1. The Reynolds averaged conservation equations for mass, momentum, and energy are solved using the volume of fluid method using ANSYS FLUENT. The turbulence is modeled using Menter's k-ω SST model with low Reynolds number correction. Khallaki et al. [16] showed that the k-ω SST model was suitable to describe the horseshoe vortex systems behind single row finned tube heat exchangers, while the previous work of Tala et al. [6] demonstrated the ability of the k-ω SST model with low Reynolds number correction to describe the thermo-hydraulic characteristics of a finned tube heat exchanger. The flow is considered incompressible with air as the working fluid and aluminum (AL1100) as the fin material. The thermo-physical properties of air were assumed to be dependent on the temperature and were obtained by curve fitting the property data over the temperature range of this study.

Symmetry boundary conditions on the surfaces shown by the lines in Figure 1 are used to reduce the computational domain. The total volume of the heat exchanger considered is $0.5 * P_t * N * P_l * F_p$ (refer to Figure 1). The computational domain is made up of three regions; (i) the heat exchanger core, (ii) the upstream and (iii) downstream regions. The inclusion of the upstream and downstream regions allows to consider the fin leading edge effect upstream of the flow and to stabilize the flow at the outlet to avoid any numerical instabilities due to the potential reversal of the flow. The upstream and downstream distances were taken to be equal to 7 times the length of the fin, which was found sufficient. Conjugate heat transfer is considered with the fin and a no-slip boundary condition is considered at all solid walls. The upstream flow is assumed uniform U_{up}, with a uniform temperature of 290K, a turbulent intensity of 3% and a turbulent viscosity ratio of $1.24U_{up.}$ A pressure outlet boundary condition is applied at the outlet. Symmetry boundary conditions are used at the symmetric planes with Y=0 and Y=0.5F_p. The main application for the flat plate and tube heat exchanger considered here is as a condenser. Thus, a convective boundary condition on the inside walls of the tube was adopted for the current simulations. Water with a saturation temperature of 75°C was assumed inside the tubes, and the heat transfer coefficient was calculated

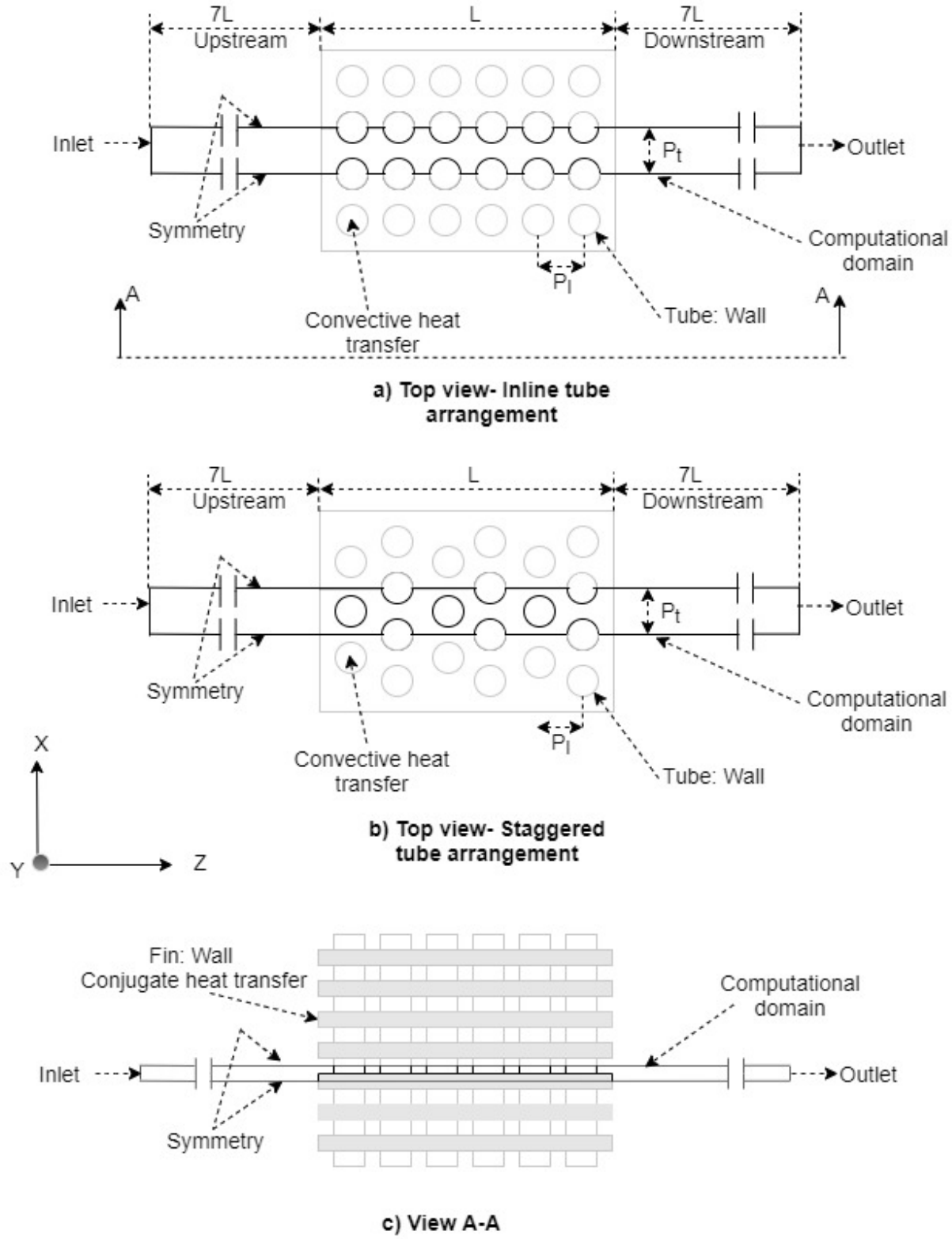

Figure 1: Details of the computational domain for a fully ducted heat exchanger.

using the correlation by Gross [17] for the laminar wavy range. The correlation yields a heat transfer coefficient of 18,000-20,000 W/m2-K. Thus, a heat transfer coefficient of 20,000 W/m2-K with a saturation temperature of 75°C was chosen for this study. The steady-state is considered for the current simulations.

Ansys meshing© was used to discretize the domain into a finite number of control volumes. The upstream and downstream are meshed with a linearly increasing mesh size. The resultant grid is shown in Figure 2. In order to study the grid independence, six grid systems having 1,578,000; 2,670,000; 3,500,000; 5,500,000; 8,500,000; 12,000,000 elements are generated for the fully ducted geometry with tube pitch of 3.5 diameters, fin pitch of 0.5 diameters and Reynolds number of 2300. For the generated grid, attention was paid to ensure that the first centroid distance to the wall had y+ <1 following the requirement of the turbulence model. The Colburn j-factor changed less than 0.2% for the grids with 5,500,000 to 12,000,000 elements. In this study, the grid with 5,500,000 is used for the simulations. Convergence was checked by monitoring the point defined just before the exit from the heat exchanger. The velocity magnitude and turbulent viscosity ratio are checked at each iteration, and the simulations are considered converged once all the residuals drop below 1e-4 and the monitored

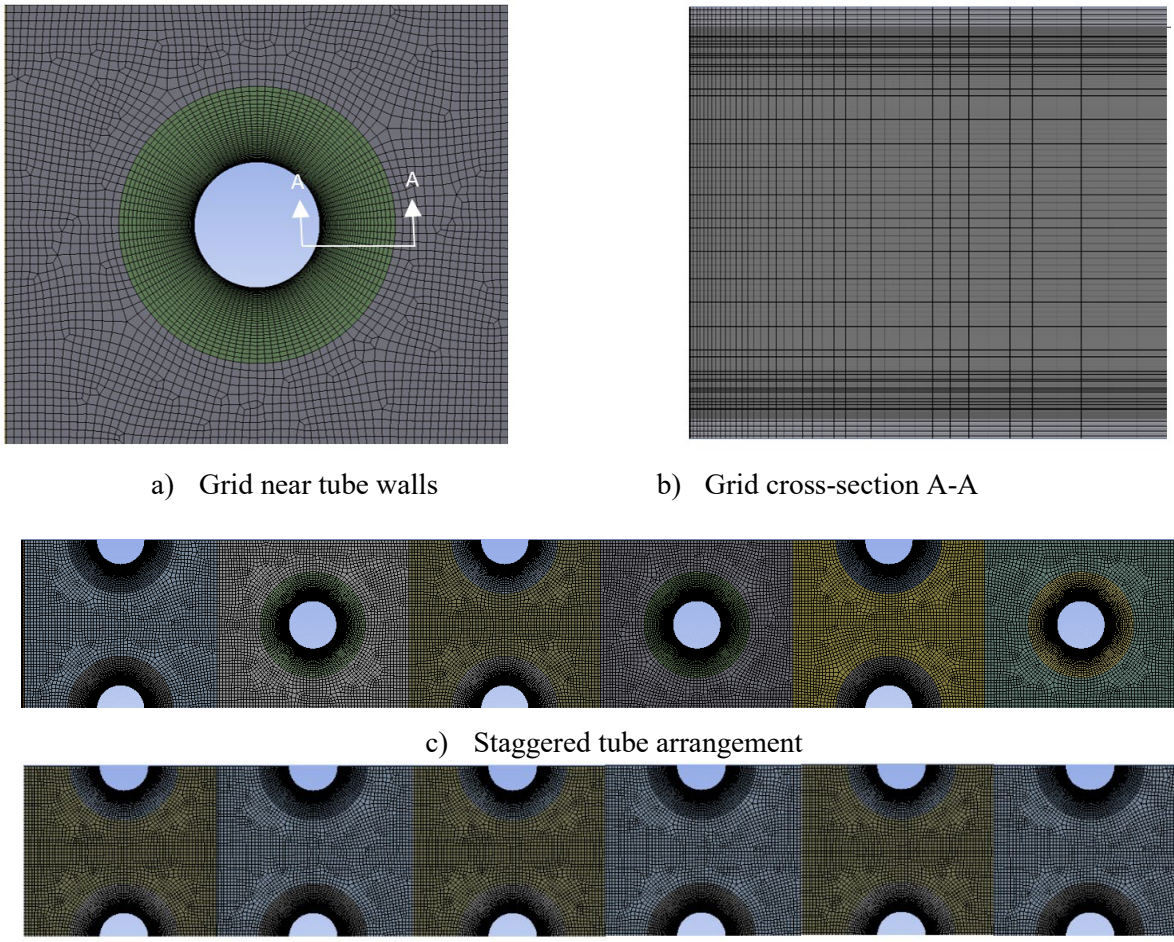

a) Grid near tube walls

b) Grid cross-section A-A

c) Staggered tube arrangement

d) Inline tube arrangement

Figure 2: Grid geometry

variable remains constant. The simulations for the inline tube arrangement were validated against the experimental data of Kim et al. [18] and for the staggered tube arrangement against the experimental correlation of Wang et al. [13]. In both cases, the numerical results were within ±10 percent of the correlations.

3. Results and discussion

Strong horseshoe vortices are seen to develop around the fin-tube junction in both the inline and staggered tube arrangements as shown in Figures 3 and 4. The streamlines on different planes around the tube with the contours of heat flux for a tube pitch of 3.5 diameters and Re_{Do}=3000 are shown here. For the inline tube geometry, the strong vortex formation can only be seen around the first tube; however, for the staggered tube arrangement, it can be seen around downstream tubes as well. The results in both cases show that the horseshoe vortex system around the first tube consists of two co-rotating primary vortices, a counter-rotating secondary vortex and a corner vortex. For the inline case, a weak second primary vortex was observed at 0° plane but not evident at a 30° plane or later. The corner vortex was observed only at 30° and 60° planes. For succeeding tubes, there is a single primary vortex on 30° planes, and the strength decreases for the next rows. For the staggered tube geometry, the horseshoe vortex system has three primary vortices, two secondary vortices and a corner vortex around the second tube. For succeeding tubes, there is a presence of the single primary vortex. However, for the last two tubes, the presence of the vortex can only be seen at a 60° plane. The primary vortex wraps around the tube from 0-90° and progressively disappears with the increase of azimuthal angle. The corner vortex is observed at 30° and 90° plane and not seen at 0° plane. A high heat flux can be found in front of the primary vortices and corner vortex.

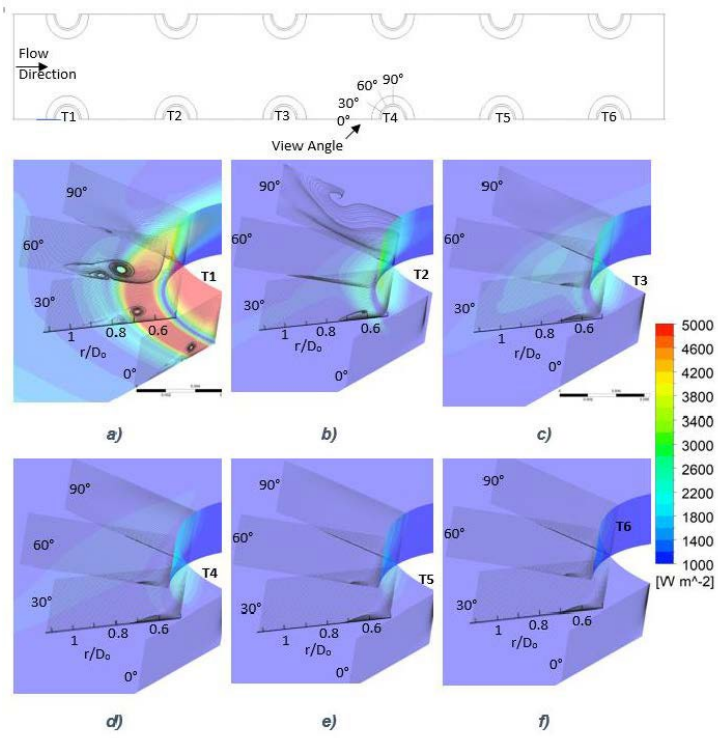

Figure 3: Horseshoe vortices around each tube for an inline geometry with tube pitch of 3.5 diameters with overlapping contours of heat flux for Re_{Do}=3000. (a) T1, (b) T2, (c) T3, (d) T4, (e) T5, (f) T6

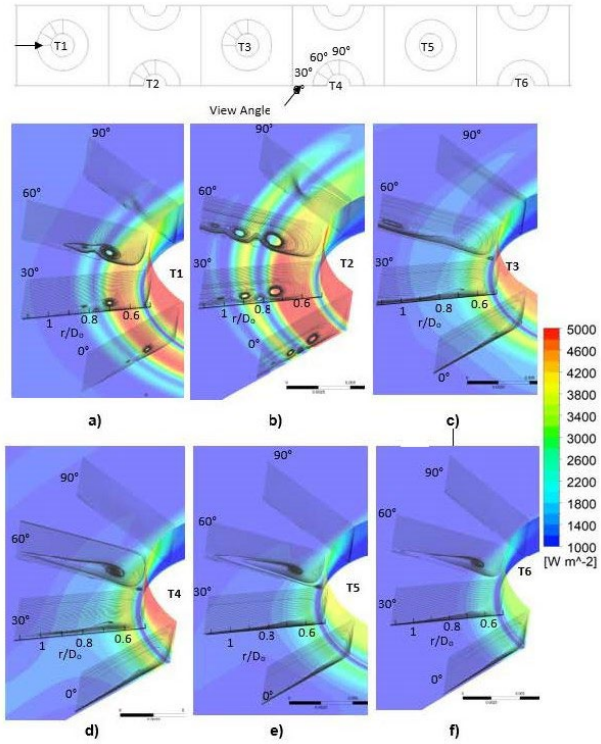

Figure 4: Horseshoe vortices around each tube for a staggered geometry with tube pitch of 3.5 diameters with overlapping contours of heat flux for Re_{Do}=3000. (a) T1, (b) T2, (c) T3, (d) T4, (e) T5, (f) T6

A total of 280 simulations were performed for the parameter space with 3 to 6 tube rows with tube pitch of 3 to 4 diameters, a fin pitch of 0.25 to 0.65 diameters and Reynolds number from 1450 to 7000. The data from these simulations were used to develop correlations for the Colburn j-factor $\left([h_o D_o/(\rho c_p U_m) Pr^{2/3}]\right)$ and friction f-factor following Wang et al. [13]. The correlation adopted for the j-factor is given by (equations 1 to 5).

$$j = C_1 * (Re_{Dc}^{P3}) * (\frac{F_P}{D_o})^{P5} * (\frac{F_P}{D_h})^{P6} * (\frac{F_P}{P_t})^{C_{13}} * N^{P4} \quad (1)$$

$$\text{P3} = C_2 + \frac{C_3 * N}{Ln(Re_{Do}^1)} + C_4 * Ln(N * (\frac{F_P}{D_c})^{C_5}) \quad (2)$$

$$\text{P4} = C_6 + \frac{C_7 * (\frac{P_1}{D_h})^{C_8}}{Ln(Re_{Do}^1)} \quad (3)$$

$$\text{P5} = C_9 + \frac{C_{10} * N}{Ln(Re_{Do}^1)} \quad (4)$$

$$P6 = C_{11} + C_{12} * Ln(\frac{Re_{Dc}^1}{N}) \quad (5)$$

and the correlation for the f-factor is given by (equations 6 to 10)

$$f = A_1 * (Re_{Do}^{P3}) * N^{P4} * (\frac{F_P}{D_o})^{P5} * (\frac{F_P}{D_h})^{P6} * (\frac{F_P}{P_t})^{A_{13}} \quad (6)$$

$$\text{P3} = A_2 + \frac{A_3 * N}{Ln(Re_{Do}^1)} + A_4 * Ln(N * (\frac{F_P}{D_o})^{A_5}) \quad (7)$$

$$\text{P4} = A_6 + \frac{A_7 * (\frac{P_1}{D_h})^{A_8}}{Ln(Re_{Do}^1)} \quad (8)$$

$$\text{P5} = A_9 + \frac{A_{10} * N}{Ln(Re_{Do}^1)} \quad (9)$$

$$P6 = A_{11} + A_{12} * Ln(\frac{Re_{Do}^1}{N}) \quad (10)$$

Multiple regression techniques using the Gauss-Newton iterative algorithm [19] were used to obtain the correlations and the coefficients from the regression analysis are provided in Tables 1 and 2. The predicted results from the correlations and original CFD data are compared in Figures 5 and 6. For the j-correlation, 98 percent of the deviations are within ±8 percent, and the root-mean-square error is around 4.3 percent. The deviations for the f-correlation are within ±10 percent, and the root-mean-square difference is around 5.4 percent.

Table 1: Coefficients for the Colburn j-correlation

C_1	C_2	C_3	C_4	C_5	C_6	C_7	C_8
1.1407	-0.5516	0.0042	0.8826	0.2769	-12.6861	40.8495	0.0499
C_9	C_{10}	C_{11}	C_{12}	C_{13}			
-2.98	0.4016	-2.2253	0.2008	0.8492			

Table 2: Coefficients for the friction factor f-correlation

A_1	A_2	A_3	A_4	A_5	A_6	A_7
24.2951	-0.6027	0.1791	0.6355	0.0538	-9.9696	26.94
A_8	A_9	A_{10}	A_{11}	A_{12}	A_{13}	
0.1036	-1.7091	0.3518	-3.573	0.3387	1.4539	

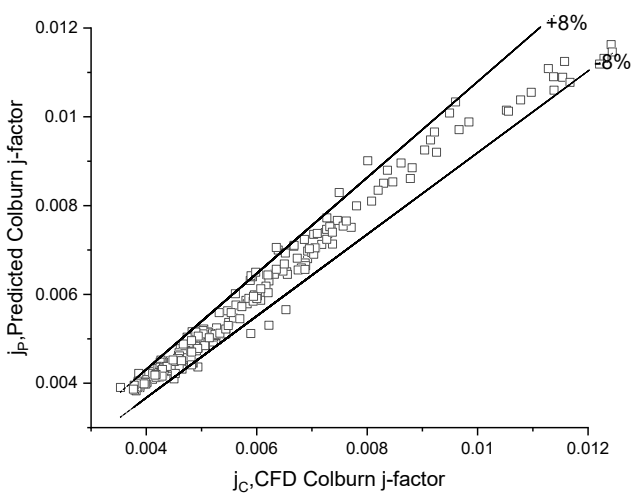

Figure 5: Comparison of heat transfer correlation with simulation data.

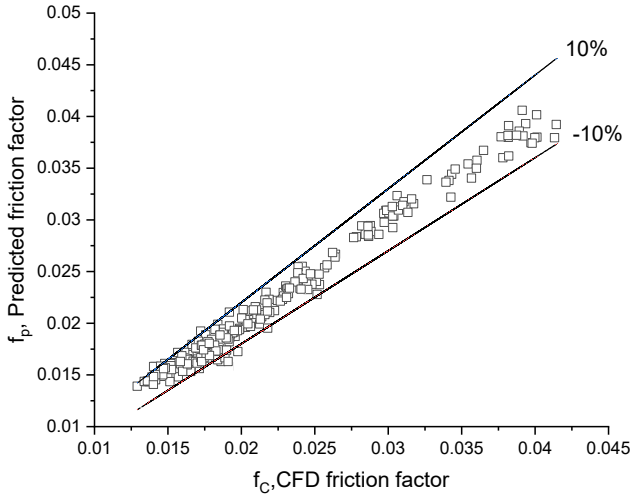

Figure 6: Comparison of friction factor correlation with simulation data

4. Conclusions

The heat transfer and pressure drop characteristics of fully ducted plate-fin and tube heat exchangers were numerically simulated. The numerical simulations were performed using the finite volume method on the commercial CFD code ANSYS FLUENT using the low Reynolds number k-ω SST turbulence model. Two heat exchanger configurations, inline and staggered tube arrangements, were considered. Strong horseshoe vortices developed around the fin-tube junction in both cases, which was associated with high heat transfer. The heat transfer and friction factor decreased significantly with the tube pitch for the staggered arrangement, but not for the inline arrangement. Correlations for the heat transfer and pressure drop for the inline configuration was developed using 280 simulations for 70 different geometric cases. The mean deviations of the correlations for the heat transfer and friction factor was of 4.3 percent and 5.4 percent, respectively.

References

[1] A. A. Bhuiyan, M. R. Amin, R. Karim and A. K. S. Islam, "Plate fin and tube heat exchanger modeling: Effects of performance parameters for turbulent flow regime," International Journal of Automotive and Mechanical Engineering, vol. 9, no. 1, pp. 1768-1781, 2014.

[2] A. A. Bhuiyan, A. S. Islam and M. Amin, "Numerical prediction of laminar characteristics of fluid flow and heat transfer in finned-tube heat exchangers," Innovative Systems Design and Engineering, vol. 2, no. 6, pp. 1-12, 2011.

[3] D.G. Rich, "The effect of fin spacing on the heat transfer and friction performance of multi-row, plate fin-and-tube heat exchangers," ASHRAE Transactions, p. 137–145, 1973.

[4] Y. Kim and Y. Kim, "Heat transfer characteristics of flat plate finned-tube heat exchangers with large fin pitch," International Journal of Refrigeration, vol. 28, no. 6, pp. 851-858, 2005.

[5] C. C. Wang, Y. J. Chang, Y. C. Hsieh and T. L. Lin, "Sensible heat and friction characteristics of plate fin-and-tube heat exchangers having plane fins," International Journal of Refrigeration, vol. 19, no. 4, pp. 223-230, 1996.

[6] J. V. S. Tala, D. Bougeard and J.-L. Harion, " Numerical analysis of the fin spacing effect on the horseshoe vortex system evolution in a two-rows finned-tube heat exchanger," International Journal of Numerical Methods for Heat & Fluid Flow, vol. 23, pp. 1136-1154, 2013.

[7] C. F. McQuiston and D. R. Tree, "Heat transfer and flow friction data for two fin–tube surfaces," ASME J. Heat Transfer, vol. 93, no. 2, pp. 249-250, 1971.

[8] D. G. Rich, "The effect of the number of tubes rows on heat transfer performance of smooth plate fin-and-tube heat exchangers," ASHRAE Trans., vol. 81, pp. 266-293, 1975.

[9] C. F. McQuiston, "Heat mass and momentum transfer data for five plate–fin–tube heat transfer surfaces," ASHRAE Trans, vol. 1, no. 84, pp. 266-293, 1978.

[10] C. F. McQuiston, "Correlation of heat, mass and momentum transport coefficients for plate-fin-tube heat transfer surfaces with staggered tubes," ASHRAE Transaction, vol. 84(1):, pp. 294-309, 1978.

[11] D. L. Gray and R. L. Webb, "Heat transfer and friction correlations for plate finned-tube heat exchangers having plain fins," in International Heat Transfer Conference Digital Library, Begel House Inc., 1986.

[12] C. C. Wang and K. Y. Chi, "Heat transfer and friction characteristics of plain fin-and-tube heat exchangers, part I: new experimental data," International Journal of Heat and Mass Transfer, vol. 43, no. 15, pp. 2681-2691, 2000.

[13] C. C. Wang, K. Y. Chi and C. J. Chang, "Heat transfer and friction characteristics of plain fin-and-tube heat exchangers, part II: Correlation," International Journal of Heat and Mass Transfer, vol. 43, no. 15, pp. 2693-2700, 2000.

[14] A. Bastani, M. Fiebig and N. K. Mitra, "Numerical studies of a compact fin-tube heat exchanger," Design and Operation of Heat Exchangers, pp. 154-163, 1992.

[15] J. Y. Jang, M. C. Wu and W. J. Chang, "Numerical and experimental studies of three-dimensional plate-fin and tube heat exchangers," International Journal of Heat and Mass Transfer, vol. 39, no. 14, pp. 3057-3066, 1996.

[16] K. Khallaki, S. Russeil, B. Baudoin, “Numerical study of the horseshoe vortex structure upstream of a single plate-finned tube,” Int. Journal of Heat and Technology, 23(1), pp.31-36, 2005.

[17] U. Gross, "Reflux condensation heat transfer inside a closed loop thermosyphon," International Journal of Heat and Mass transfer, vol. 35, no. 2, pp. 279-294, 1992.

[18] N. H. Kim, B. Youn and R. L. Webb, "Air-side heat transfer and friction correlations for plain fn-and-tube heat exchangers with staggered tube arrangements," Journal of Heat Transfer, vol. 121, no. 3, p. 662, 1999.

[19] G. A. F. Seber, Nonlinear Regression, The Wiley-Interscience Paperback Series, 2015, pp. 117-128.